Proceedings of 20th International Congress on Acoustics, ICA 2010
23-27 August 2010, Sydney, Australia

A Study on Acoustic Theoretical Formulae for Compact Acoustic Reproduction Systems

Masashi Nakamura (1), Yoshinobu Kajikawa (1), Yasuo Nomura (1) and Takashi Miyakura (2)

(1) Faculty of Engineering Science, Kansai University, 3-3-35, yamatecho, Suita-shi, Osaka, Japan
(2) Hosiden Corporation, 1-4-33 Kitakyuhoji, Yao-shi, Osaka, Japan

PACS: 43.38.-p Transduction; acoustical devices for the generation and reproduction of sound

ABSTRACT

In this paper, we propose a method for analyzing compact acoustic reproduction systems (e.g. mobile phones) through acoustic equivalent circuits. Measured responses of compact acoustic reproduction systems cannot be represented accurately by the analysis based on the conventional acoustic theory. Acoustic engineers consequently are obliged to design compact acoustic reproduction systems by trial and error. Moreover, the sound quality of those systems is likely to deteriorate due to the difficulty of such an acoustic design. We therefore clarify the cause of the difference between the measured response and the analysis one calculated by the finite element method (FEM) analysis and consider the possibility of obtaining new acoustic theorical formulae based on the analysis results in order to make it easier for acoustic engineers to design compact acoustic reproduction systems.

INTRODUCTION

Recently, the demand for small, thin acoustic reproduction systems (e.g. mobile phones) has been increasing. The acoustic structure design for mobile phones is becoming more and more difficult because the mobile phones are made smaller and more complicated. As a result, even experienced engineers design compact acoustic reproduction systems by the trial and error. The trial and error design increases cost, wastes time, and deteriorates the sound quality. To solve this problem, we proposed an automatic design technique using genetic algorithm (GA) for the acoustic components of mobile phones [1]. This system is based on the acoustic equivalent circuit analysis using the conventional acoustic formulae. However, this system is impractical because it cannot describe the variation of acoustic parameters related to the spatial relationship of acoustic holes. To solve this problem, we have already examined the influence of the spatial relationship between acoustic holes using two dimensional FEM analysis [2], [3]. However, the physical mechanism has not been clarified enough. We therefore analyze an actual acoustic phenomenon using three dimensional FEM analysis, and clarify the cause through the analysis results. Moreover, we discuss the possibility of new acoustic theorical formulae based on the analysis results.

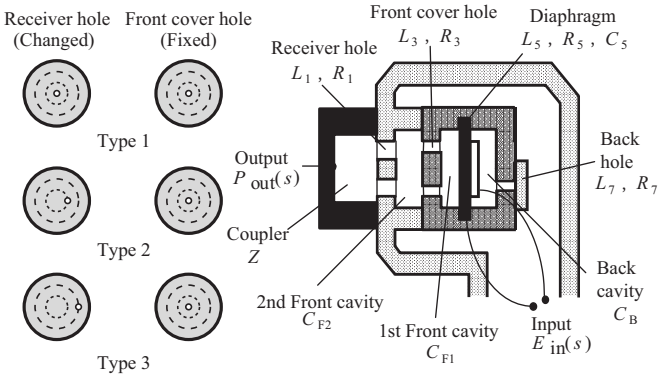

Figure 1. Structure of a mobile phone.

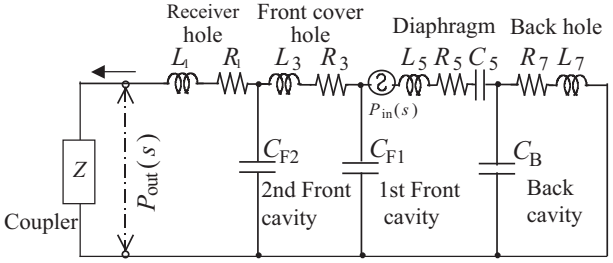

Figure 2. Equivalent circuit model of Fig. 1.

CONVENTIONAL ACOUSTIC FORMULAE FOR ACOUSTIC HOLE AND THEIR PROBLEM

The general acoustic formulae for acoustic hole are given depending upon the frequency range as follows [4]:

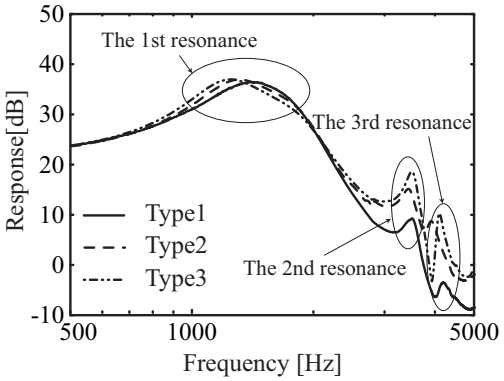

(a) Measured characteristic

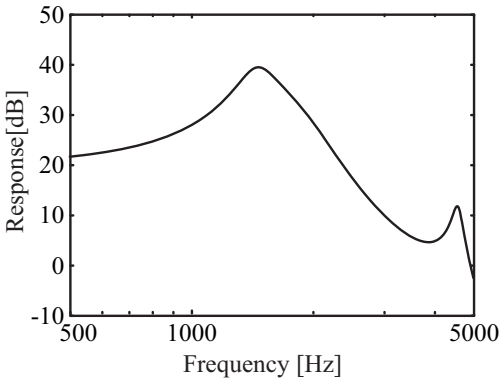

(b) Simulated characteristic

Figure 3. Comparison of measured frequeny responses of Fig. 1 and the corresponding simulated frequency ones calculated by the conventional acoustic theory.

Table 1. Sizes and acoustic parameters of Fig. 1.

		Parameter
Diaphragm (R_5 , L_5 , C_5)	R_5	2.76×10^{7}
	L_5	3.56×10^{3}
	C_5	4.67×10^{-12}
Receiver hole (R_1 , L_1)	Length	1.6
	Radius	1.0
	Number	1
2nd front cavity (C_{F1})	Capacity	3.30
Front cover hole (R_3 , L_3)	Length	0.3
	Radius	1.35
	Number	1
1st front cavity (C_{F2})	Capacity	0.43
Back cavity (C_B)	Capacity	0.56
Back hole (R_7 , L_7)	Length	1.0
	Radius	0.9
	Number	1

Length[mm], Radius[mm], Capacity[cc]

・ $a < 0.002/\sqrt{f}$

$$R_1 = 8\pi\frac{\mu h}{NS^2}, L_1 = \frac{4}{3}\frac{\rho_0 h}{NS} \tag{1}$$

・ $0.01/\sqrt{f} < a < 10/f$

$$R_2 = \frac{\rho_0\sqrt{2\omega\mu}}{NS}\left[\frac{h}{a}+2\right] \tag{2}$$

$$L_2 = \frac{\rho_0}{NS}\left[h+2l\right] \tag{3}$$

・ $0.002/\sqrt{f} < a < 0.01/\sqrt{f}$

$$Z_3 = Z_1\frac{0.01/\sqrt{f}-a}{0.008/\sqrt{f}} + Z_2\frac{a-0.002/\sqrt{f}}{0.008/\sqrt{f}} \tag{4}$$

$$Z_1 = R_1 + j\omega L_1, Z_2 = R_2 + j\omega L_2 \tag{5}$$

where Z_1, Z_2 and Z_3 is acoustic impedance of acoustic hole in pascal・second per cubic meter, R acoustic resistance of acoustic hole in pascal・second per cubic meter, L acoustic mass in pascal・square second per cubic meter. h length of acoustic hole in meters, a radius of holes in meters, l length of open-end correction in meters, ρ_0 air density in kilogram per cubic meter, N number of acoustic holes, μ viscosity coefficient of air in pascal・second, and S cross sectional area of acoustic holes in square meter.

Fig. 1 shows the acoustic structure of a mobile phone, whose sizes and acoustical equivalent circuit are shown in Table 1 and Fig. 2, respectively. Fig. 3 shows measured responses and the corresponding calculated ones obtained by the conventional acoustic formulae in case where the position of the receiver hole changes as shown in Fig. 1. From Fig. 3(a), we can see that the level of the response becomes high as the position of the receiver hole moves outwardly from the center of the receiver plane. On the other hand, the calculated response shown in Fig. 3(b) cannot explain the change of measured responses at 2nd and 3rd resonant frequencies. Hence, the conventional acoustic formulae are useless to practical design. In the next section, we clarify the causes through some analyses by FEM analysis.

ACOUSTICAL PHENOMENON ANALYSIS USING FINITE ELEMENT METHOD

Fig. 4 shows the structure of a mobile phone, whose sizes and acoustical equivalent circuit are shown in Table 2 and Fig. 5, respectively. We analyze the acoustic phenomenon of this structure by the finite element mothod (FEM), especially, including acoustic impedance analysis.

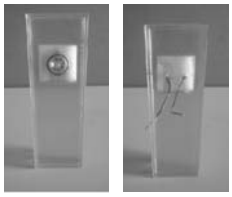

(a) External

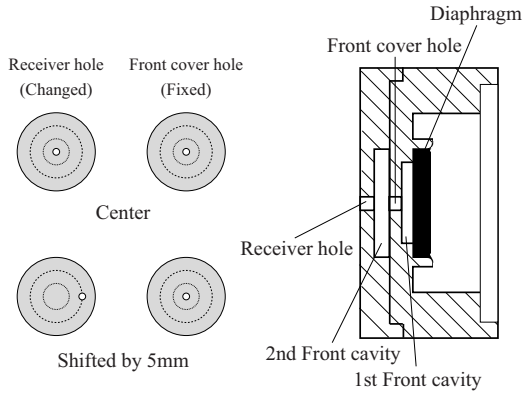

(b) Stracture

Figure 4. Prototype of a mobile phone.

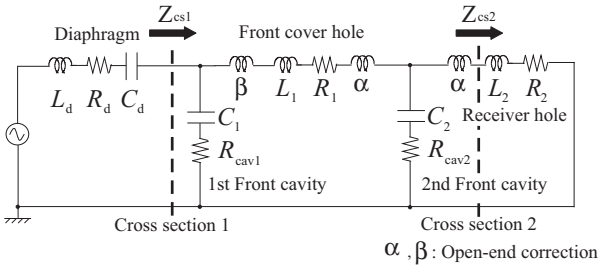

Figure 5. Equivalent circuite model of Fig. 4.

In this simulation, the model shown in Fig. 6 is used. The boundary condition on the inside wall is set as the particle velocity is equal to 0. Additionally, the boundary condition on the output edge is set as the sound pressure is equal to 0. The simulation conditions are shown in Table 3.

Input signal

In this simulation, the virtual plane sound source in Fig. 6 is driven by an input signal (particle velocity) $u_{vps}(t)$ which is a gaussian pulse as follows [5]:

$$u_{vps}(t) = A_0 e^{-\{(\Delta tn - T)/0.29T\}^2} \tag{6}$$

where Δt is sampling period, n integer, t ($t = \Delta tn$) time, A_0 amplitude, and T is determined according to the frequency f_0 at which the electric power spectrum of the gaussian pulse decreases by 3dB as follows:

$$T = 0.646 / f_0 \tag{7}$$

Fig. 7 shows the dynamics of gaussian pulse used for the analysis, whose parameters and electric power spectrum are shown in Table 4 and Fig. 8, respectively.

Table 2. Sizes and acoustic parameters of Fig. 4.

		Parameter
Diaphragm (HDR9310) (R_d , L_d , C_d)	R_d	8.14×10^{6}
	L_d	8.91×10^{3}
	C_d	4.02×10^{-12}
Receiver hole (R_2 , L_2)	Length	1.0
	Radius	1.0
	Number	1
1st front cavity (C_1)	Capacity	0.18
Front cover hole (R_3 , L_3)	Length	1.0
	Radius	1.0
	Number	1
2nd front cavity (C_2)	Capacity	$64\pi h\times10^{-3}$

Length[mm], Radius[mm], Capacity[cc]

Table 3. Simulation conditions.

Type of fluid	Air (incompressible)
Specific heat ratio	1.4
Temperature	20℃
Viscosity of air	18.2E-6Pa・s

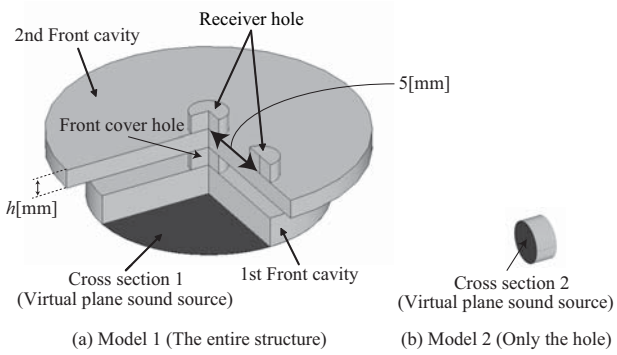

(a) Model 1 (The entire structure) (b) Model 2 (Only the hole)

Figure 6. Model of simulation with FEM analysis.

Acoustic impedance analysis

The sound pressure in the structure is caused by the particle velocity at the virtual plane sound source in Fig. 6. At that time, the sound pressure p_{vps} at the virtual plane sound source is calculated by the FEM analysis and the acoustic impedance Z_{vps} of the output edge side to the virtual plane sound source can be calculated by

$$Z_{vps}(\omega) = \frac{P_{vps}(\omega)}{S \cdot U_{vps}(\omega)}, \tag{8}$$

where S is the area of the virtual plane sound source.

Table 4. Parameters of gaussian pulse.

A_0	1.0E-5
Δt	1.0E-5sec
f_0	10.0kHz

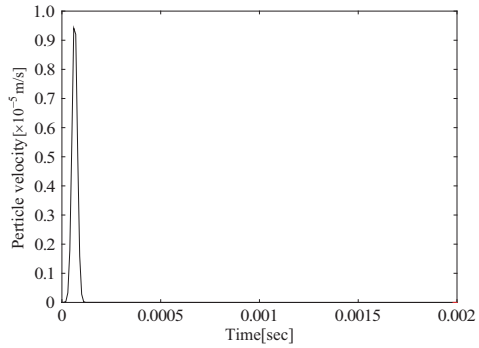

Figure 7. Dynamics of gaussian pulse.

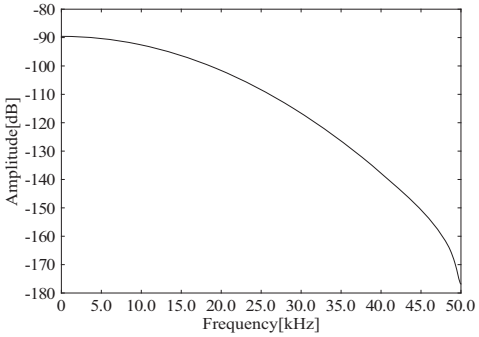

Figure 8. Amplitude-Frequency characteristic of gaussian pulse.

Procedure for estimating acoustic parameters

In this simulation, acoustic impedance analyses are done on the two kinds of structures shown in Fig. 6. To clarify how the acoustic parameter of the receiver hole changes according to the position, the acoustic parameters shown in Fig. 5 are estimated.

First of all, Model 1 shown in Fig. 6 is considered. From Fig. 5, we can see that the acoustic compliance of the cavity is considered to be open at low frequencies because the acoustic impedance of the cavity grows very much. Therefore, the acoustic impedance at low frequencies can be approximated as follows:

$$Z_{cs1} \approx (R_1 + R_2) + j\omega(L_1 + L_2 + 2\alpha + \beta) \quad (9)$$

(Low frequency band)

In a word, the gradient of the reactance to the angular frequency shows the sum total of the acoustic mass M_t $(M_t = L_1 + L_2 + 2\alpha + \beta)$. Hence, the sum total of the acoustic mass M_t can be estimated.

Next, the analysis of Model 2 is described. The acoustic impedance Z_{cs2} in Model 2 is shown as follows:

$$Z_{cs2} = R_2 + j\omega L_2 \quad (11)$$

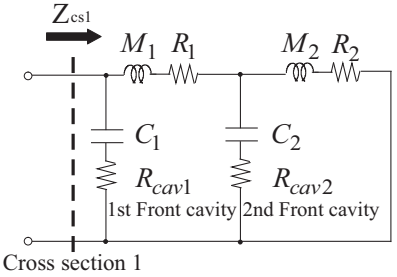

Figure 9. Equivalent circuit model of Model 1.

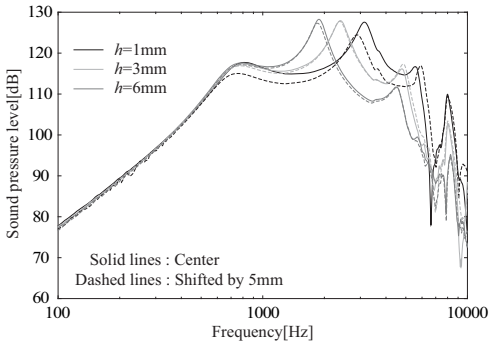

Figure 10. Measured frequency characteristics in case where the position of the receiver hole changes (SPL).

Therefore, R_2 can be estimated from real part and L_2 can be estimated from the gradient of the reactance to the angular frequency.

To finally estimate other parameters, the equivalent circuit shown in Fig. 9 to Model 1 is employed. M_1 and M_2 in Fig. 9 are defined as follows:

$$\begin{aligned} M_1 &= L_1 + \alpha + \beta \\ M_2 &= L_2 + \alpha \\ (M_t &= M_1 + M_2) \end{aligned} \quad (10)$$

The parameters shown in Fig. 9 are determined by the relationship between the acoustic impedance characteristics based on the equivalent circuit analysis and the FEM analysis. Specifically, these parameters are determined to become small most the sum total of square error of characteristics based on the equivalent circuit analysis and the FEM analysis by Maximum Likelihood Estimation (MLE). In addition, since the receiver hole and the front cover hole are the same sizes, $R_1 = R_2$ and $L_1 = L_2$. Therefore, all parameters of Model 1 are determined. However, it is difficult to estimate those parameters accurately because there are a lot of the combinations of the parameters to match both characteristics.

ANALYSIS RESULTS

Fig. 10 shows the measured frequency characteristics of a mobile phone shown in Fig. 4. From Fig. 10, we can see that the frequency characteristics vary according to the position of the receiver hole. In this section, such a phenomenon is clarified based on some analysis results.

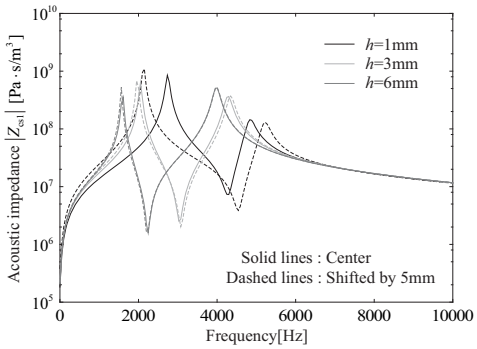

Figure 11. Acoustic impedance charasteristics in case where the position of the receiver hole changes (Model 1).

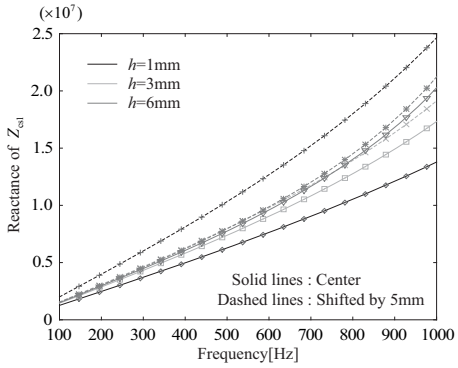

Figure 12. Reactance characteristics in case where the position of the receiver hole changes (Model 1).

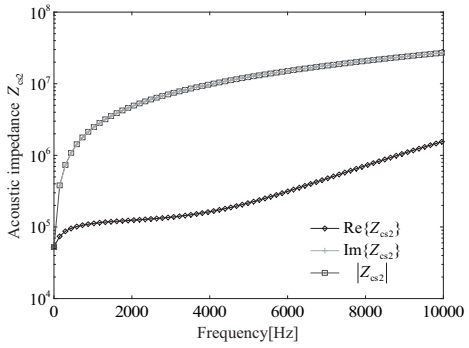

Figure 13. Acoustic impedance charasteristics (Model 2).

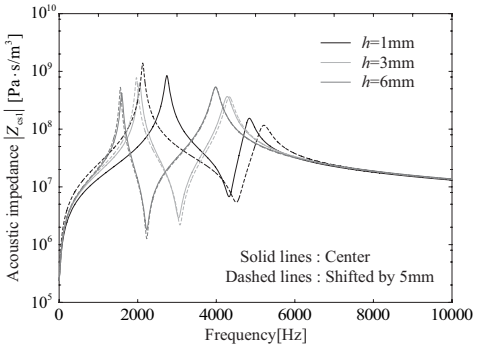

Figure 14. Acoustic impedance characteristic that uses estimated parameters.

Acoustic impedance analysis

- **Model 1**

Fig. 11 shows the acoustic impedance characteristics of Z_{cs1} in Model 1 by the FEM analysis. From Fig. 11, it can be seen that the position of the receiver hole influences the acoustical characteristics. Moreover, the influence grows as the height of the 2nd front cavity becomes short. The measured characteristics shown in Fig. 10 also have the same tendency. Next, Fig. 12 shows the reactance characteristics of Z_{cs1}. Fig. 12 shows that the resonant frequency changes according to the sum total of the acoustic mass, and influences the acoustic characteristics. The gap between the front cover hole and the receiver hole relates to the increase of the acoustic mass in the tight space. The cause is examined in detail in the next section.

- **Model 2**

Fig. 13 shows the acoustic impedance characteristics of Z_{cs3} in Model 3 by the FEM analysis. From Fig. 13, we can see that the resistance is a function of the frequency. However, the change is small compared with that of the reactance, so that the resistance is treated as a parameter that does not depend on the frequency. Therefore, the acoustic resistance R_1 is regarded as a mean value.

Estimated result of acoustic parameters

Fig. 14 shows acoustic impedance characteristics that use the estimated parameters. From Fig. 14, we can see that these characteristics are consistent with the characteristics obtained from the FEM analysis. Hence, it can be seen that the parameters can be estimated accurately.

Next, Figs. 15-17 show parameters estimated by MLE. From Fig. 15, it can be seen that the sum total of the acoustic mass M_t increases as the position of the acoustic hole shifts from center to edge. Furthermore, the increase is remarkable as the 2nd front cavity narrows. This is because a virtual tube is formed by the open-end correction in the 2nd front cavity and the interference becomes intense as the the 2nd front cavity narrows. From Fig. 16, we can see that there is little influence of the position of the acoustic hole and these parameters are almost the same value as the theory ones. Hence, we can see that the variation of the acoustic characteristics according to the position of the receiver hole is related to the change in the acoustic mass. Next, R_{cav1} and R_{cav2} shown in The parameters shown in Fig. 17 cannot be calculated by the conventional acoustic theory. This is because the viscosity of air becomes large as the space of the cavity narrows. Therefore, the resistance of the 1st cavity whose capacity does not change is a constant and the resistance of the 2nd cavity whose capacity changes grows as the space of the cavity narrows.

From the analysis results, the formulae that accurately calculate the open-end correction and the related resistance should be established for the compact acoustic reproduction systems such as mobile phones because the acoustic characteristics change according to the position of the acoustic hole.

CONCLUSIONS

In this paper, we have examined the influence of the position of the acoustic hole to the acoustic characteristics based on three dimensional FEM analysis. As a result, we need to consider the change in the open-end correction and that in the acoustic resistance of the narrow cavity depending on the position of the acoustic hole in case where compact acoustic reproduction systems are designed.

In the future, we will obtain the acoustic theorical formulae that can explain the measurement characteristic accurately from various analysis results.

REFERENCES

1 Y. Nomura, T. Nakatani, Y. Kajikawa, “An Automatic Design Technique Using Genetic Algorithm for the Acoustic Component of Mobile Phones”, 17th International Congress on Acoustics, Rome, Italy, Sep. 2001.

2 Y. Nagase, S. Tsujikawa, Y. Kajikawa, Y. Nomura, “A Method for Analyzing Compact Acoustic Reproduction Systems through Acoustic Equivalent Circuit”, 19th International Congress on Acoustics, Madrid, Spain, Sep. 2007.

3 Y. Nagase, Y. Kajikawa, Y. Nomura, “A Study on Effects the Relative Position of Acoustic Holes in Acoustic Equivalent Circuit Analysis”, IEICE Technical Report EA, vol. 107, no. 470, pp. 13-17, Osaka, Japan, Jan. 2008.

4 Leo L. Beranek, Acoustics, McGraw-Hill Book Company, 1954.

5 O. Hashimoto, T. Abe, Finite-difference time-domain method, Morikita Publishing Co., Ltd., Japan, 2006., In Japanese.

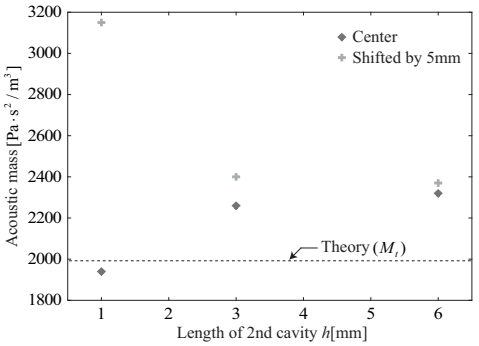

Figure 15. Estimated parameter M_t .

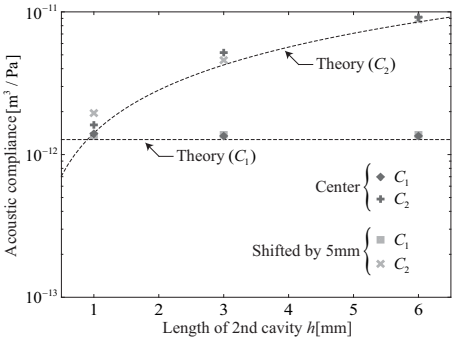

Figure 16. Estimated parameters C_1 and C_2 .

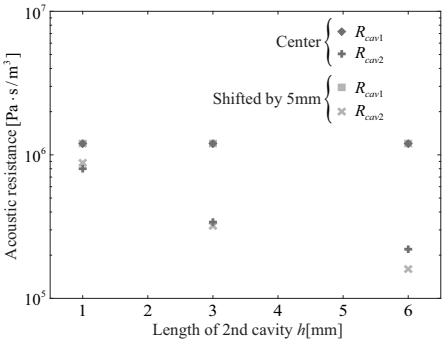

Figure 17. Estimated parameters R_{cav1} and R_{cav2} .